PHYSICAL REVIEW A, VOLUME 63, 063810

Generalized Einstein *B* coefficients for coherently driven three-level systems

J. Mompart and R. Corbalán
Departament de Física, Universitat Autònoma de Barcelona, E-08193 Bellaterra, Spain
(Received 28 April 2000; published 11 May 2001)

Generalized Einstein *B* coefficients for coherently driven closed three-level systems are introduced by means of the quantum-jump technique. The nonreciprocity between stimulated emission and absorption for both one-photon and two-photon gain and loss processes has been studied and quantified in terms of the rates of the particular incoherent processes present in each three-level system. Some general properties of these generalized Einstein *B* coefficients have been found. In particular, whenever the generalized Einstein *B* coefficient for one-photon gain overcomes that for one-photon loss then the generalized Einstein *B* coefficient for two-photon loss overcomes that for two-photon gain, and vice versa. Finally, we have obtained simple analytical expressions indicating the way to maximize the asymmetry between stimulated emission and absorption coefficients either for one-photon or for two-photon processes.

DOI: 10.1103/PhysRevA.63.063810 PACS number(s): 42.50.Gy, 32.80.−t

I. INTRODUCTION

The combination of Bohr's atomic model with a stochastic conception of the light-matter interaction allowed Einstein (1916-1917) to determine, in the context of his study of blackbody radiation, the relationship between the rates of absorption and stimulated emission of light by a gas atom possessing discrete energy levels, in terms of the so-called Einstein *B* coefficients [1]. In the framework of perturbation theory, equal *B* coefficients for absorption and stimulated emission between two nondegenerate levels were obtained. These coefficients together with the Einstein *A* coefficient accounting for spontaneous emission allowed Einstein to establish rate equations governing the atomic populations and light propagation through an atomic medium. Thus, according to Einstein theory, the atomic population differences determine the light attenuation or amplification by the atomic medium. In particular, as is shown in any standard laser textbook, the equality between stimulated emission and absorption *B* coefficients implies the well known population inversion condition for light amplification.

Nevertheless, this preliminary picture of the light-matter interaction in terms of the Einstein coefficients no longer holds in the presence of a nonperturbative interaction such as that produced by a laser field. In this case, the Schrödinger equation must be solved nonperturbatively for a suitable description of the interaction with the laser field. Unfortunately, a pure Schrödinger evolution does not succeed in describing the irreversibility associated with dissipation, e.g., in the presence of spontaneous emission. The Schrödinger equation can no longer describe, in general, the dynamics of a system consisting of an atom in interaction with a coherent field and subjected to dissipative processes.

In the presence of both coherent and incoherent processes, the standard procedure is the application of Langevin theory to the quantum mechanical system, resulting in a theory that generalizes the Einstein and Schrödinger approaches. This results in a reduced density matrix that gives a quantitative description of the behavior of the system but does not provide, in general, a clear physical interpretation of the particular mechanisms involved in the light-matter interaction. In the presence of intense laser fields, the density-matrix formalism suggests, for instance, that light amplification or attenuation by the medium is no longer determined by the population differences alone, which, in turn, suggests a nonequality between the probabilities of the reverse processes of stimulated emission and absorption.

For many years, different efforts have been made to decompose the reduced density-matrix evolution into pure state evolution. In the last decade, different stochastic decompositions of the density-matrix were proposed based on the interplay of a Schrödinger evolution accounting for the continuous evolution associated with the coherent interaction, and wave-function collapses or quantum jumps associated with dissipation [2–5]. Recalling Einstein theory, all these approaches were based on a stochastic conception of the light-matter interaction to describe dissipation. Thus, the time evolution of the wave function of a single atom, a so-called quantum trajectory, consists of a series of continuous coherent evolution periods separated by quantum jumps or wave-function collapses occurring at random times. The continuous evolution is calculated by intregrating the Schrödinger equation using an effective non-Hermitian Hamiltonian while quantum jumps occurring at random times account for the irreversibility associated with dissipation. This quantum-trajectory formalism, which is indeed equivalent to the usual description in terms of optical Bloch equations when averaged over many realizations of the trajectories, is interesting for at least two different reasons: (i) in the wave-function treatment of a system belonging to an *N*-dimensional Hilbert space the number of variables is *N* while in the density matrix it is N^2, and (ii) it provides new insights into the underlying physical mechanisms involved in the light-matter interaction. In fact, the quantum-trajectory approach has been applied with success to a large number of problems in quantum optics [6,7].

Based on the quantum-trajectory formalism and using the method of delay functions [8] previously introduced to study the fluorescence of single atomic systems, Cohen-Tannoudji *et al.* [7] derived general statistical properties of the coherent evolution periods occurring between two successive quantum jumps. These statistical tools provide, without the neces-

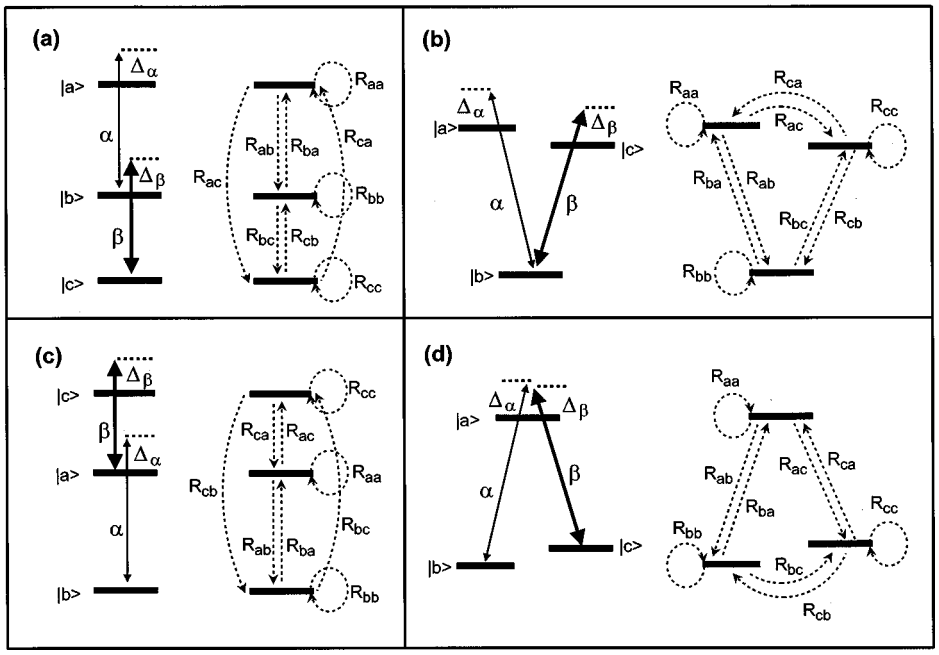

FIG. 1. Closed three-level systems under investigation: (a) *h*, (b) V, (c) *p*, and (d) Λ schemes. α and Δ_α (β and Δ_β) are the Rabi frequency and detuning of the probe (driving) TW laser field. The rates R_{ij} with $i,j=a,b,c$ account for the incoherent processes present in each particular scheme.

sity of explicitly performing a quantum-trajectory or Monte Carlo simulation, (semi)analytical expressions for the contribution of the different physical processes responsible for the attenuation or amplification of a laser field in interaction with an atomic medium. For these techniques to be applicable, two conditions are required: (i) the number of relevant atomic states involved in dissipative processes has to be finite, and (ii) the Hamiltonian has to be time independent. Using these statistical tools, Arimondo [9] and Cohen-Tannoudji *et al.* [7] revealed that inversionless amplification in the so-called V- and Λ-type three-level systems results from the fact that, for appropriate parameter values, two-photon gain processes overcome one- and two-photon loss processes even with population inversion at neither the one-photon transition nor the two-photon transition. On the contrary, one-photon gain is the physical process responsible for inversionless amplification in cascade three-level systems [10,11], also with neither one- nor two-photon population inversion [12]. In addition, Carmichael [13] has recently presented an extensive analysis of the origin of inversionless gain in the V scheme where lasing without inversion was observed for the first time [14]. Finally, these techniques have also allowed an explanation of inversionless amplification in terms of the quantum Zeno effect [15].

In this paper, we will use the statistical tools developed by Cohen-Tannoudji and co-workers [7] to introduce generalized Einstein *B* coefficients for one- and two-photon gain and loss processes in coherently driven three-level systems. These coefficients will allow us to quantify in simple analytical expressions the nonreciprocity between stimulated emission and absorption for one- and two-photon processes. Some general properties of the asymmetry between the generalized Einstein *B* coefficients for both one-photon processes and two-photon processes will be obtained. Finally, some indications to maximize these asymmetries in terms of the rates of the incoherent processes present in each scheme will be given.

Section II introduces the coherently driven closed three-level systems under investigation and reviews the quantum-jump technique used to describe the interaction of these three-level systems with laser fields in the presence of dissipation. Thus, by using the quantum-jump formalism, generalized Einstein *B* coefficients for one- and two-photon gain and loss processes are defined in Sec. III. Section IV discusses some general properties of these generalized Einstein *B* coefficients. Finally, the main results of this paper are summarized in the Conclusions.

II. MODEL AND REVIEW OF THE QUANTUM-JUMP FORMALISM

Let us consider the four closed three-level schemes shown in Fig. 1 which, in the following, we will call as *h* [Fig. 1(a)], V [Fig. 1(b)], *p* [Fig. 1(c)], and Λ [Fig. 1(d)]. In each of these schemes a weak traveling wave (TW) probe laser with Rabi frequency α and detuning $\Delta_\alpha=\omega_\alpha-\omega_{ab}$ couples to transition $|a\rangle$-$|b\rangle$ while an intense TW laser field with Rabi frequency β and detuning Δ_β drives the adjacent transition. Dissipative processes are described by means of the population transfer rates R_{ij} with $i,j=a,b,c$. Thus, R_{ij} with $i\neq j$ accounts for, e.g., spontaneous emission, incoherent pumping, or inelastic collisions transferring atoms from level $|i\rangle$ to level $|j\rangle$, while R_{ii} describes dipole dephasing due to, e.g., elastic collisions or finite laser linewidth [16]. Although initially R_{ij} with $i\neq j$ can account only for one-way incoherent pumping processes, it is straightforward to describe bidirectional pumping in these schemes. For instance, let us denote by Λ the rate of a bidirectional pumping process coupled to transition $|a\rangle$-$|b\rangle$ for the *h* scheme of Fig. 1(a); then $R_{ab}=\Lambda+\gamma_{ab}$ and $R_{ba}=\Lambda$ with γ_{ab} the spontaneous emission rate from $|a\rangle$ to $|b\rangle$.

In what follows, let us consider a quantum description of both laser fields, where N_α and N_β are the photon numbers of probe and drive laser modes, respectively. In the quantum-

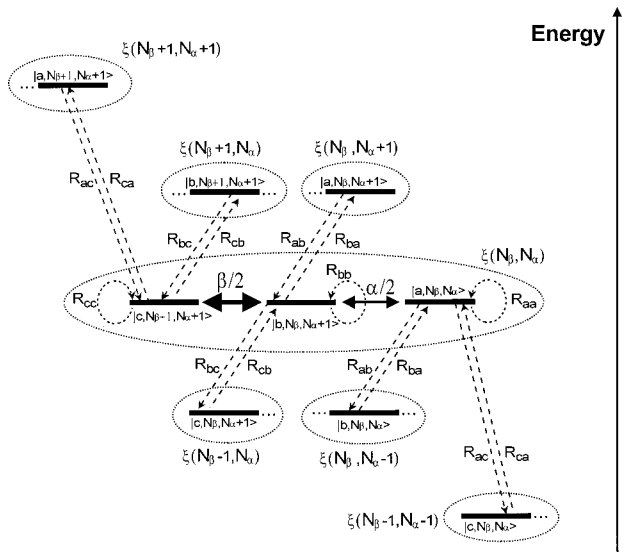

FIG. 2. Different manifolds $\xi(N_\beta \pm m, N_\alpha \pm n)$ of the three (quasi)degenerate states of the total system (atom plus laser fields) for the *h* scheme of Fig. 1(a). N_α and N_β are the photon numbers in the probe and driving modes, respectively. The solid horizontal arrows represent the continuous evolution given by the laser interaction, while the dashed oblique and circular arrows represent the quantum jumps produced by the dissipative processes.

jump formalism, the time evolution of the total system (atom plus laser fields), a so-called quantum trajectory, is calculated by integrating the time-dependent Schrödinger equation using an effective non-Hermitian Hamiltonian. Incoherent processes produce random quantum jumps that collapse the wave function to a single state. Thus a quantum trajectory consists of a series of coherent evolution periods separated by quantum jumps occurring at random times.

To be specific, Fig. 2 shows, for the *h* scheme of Fig. 1(a), the states of the total system (atom plus laser photons) grouped into different manifolds, the elliptical regions denoted by ξ, of three (quasi)degenerate states:

$$\xi(N_\beta+m,N_\alpha+n) \equiv \begin{cases} \{|a,N_\beta+m,N_\alpha+n\rangle \\ |b,N_\beta+m,N_\alpha+1+n\rangle \\ |c,N_\beta+1+m,N_\alpha+1+n\rangle\}, \end{cases} \quad (1)$$

with $m,n=0,\pm 1,\pm 2,\ldots$. In this figure, the different manifolds are displayed from bottom to top according to the increase in the total energy of the system with the assumption $|\omega_\alpha-\omega_\beta| \ll \omega_\alpha,\omega_\beta$. The horizontal solid arrows represent the laser interaction while the oblique and circular dashed arrows account for dissipative processes. After a quantum jump has just occurred, the system starts its evolution in one state of some manifold and, due to the interaction with the laser fields, evolves continuously between the three states of the given manifold in a Rabi oscillatory fashion. This coherent evolution lasts until a quantum jump associated with some kind of dissipation interrupts the continuous evolution. As a general feature, dissipative processes associated with R_{ij} with $i \neq j$ correspond to quantum jumps connecting different manifolds while those associated with R_{ij} with $i=j$ yield a new coherent evolution period in the same manifold as the previous one [16]. After the quantum jump occurs, the continuous evolution resumes again. An illustrative example of a quantum trajectory could be, for instance,

$$\cdots \xrightarrow{R_{bc}} \xi(N_\beta-1,N_\alpha-1) \xrightarrow{R_{ca}} \xi(N_\beta,N_\alpha)$$

$$\xrightarrow{R_{bb}} \xi(N_\beta,N_\alpha) \xrightarrow{R_{bc}} \xi(N_\beta-1,N_\alpha) \xrightarrow{R_{ab}} \cdots .$$

Let us now label the continuous coherent evolution periods between two successive quantum jumps, which will be called period (i,j), by the atomic state $|i\rangle$ in which the system starts the coherent evolution and the atomic state $|j\rangle$ from which the quantum jump takes place at the end of this period. Then, a stochastic quantum trajectory has the general form

$$\cdots R_{ij}\text{period}(j,k)R_{kl}\text{period}(l,m)R_{mn}\cdots,$$

with $i,j,k,l,m,n=a,b,c$. In all closed three-level systems under investigation, there are up to nine possible coherent evolution periods. These periods are characterized by well-defined changes in the laser field photon number although only in four of them does the probe photon number change. In particular, for the *h* and V schemes of Figs. 1(a) and 1(b) these four coherent evolution periods involving a change $\Delta N_\alpha = \pm 1$ in the number of probe photons are

$$\text{period}\,(a,b) \rightarrow \Delta N_\alpha = +1, \quad \Delta N_\beta = 0 \rightarrow \text{one-photon gain},$$

$$\text{period}(b,a) \rightarrow \Delta N_\alpha = -1, \quad \Delta N_\beta = 0 \rightarrow \text{one-photon loss},$$

$$\text{period}(a,c) \rightarrow \Delta N_\alpha = +1,$$

$$\Delta N_\beta = +1 \rightarrow \text{two-photon gain},$$

$$\text{period}(c,a) \rightarrow \Delta N_\alpha = -1, \quad \Delta N_\beta = -1 \rightarrow \text{two-photon loss}.$$

Two different probe gain (loss) processes are therefore identified in the quantum-jump formalism. A coherent evolution starting in $|a\rangle(|b\rangle)$ and ending in $|b\rangle(|a\rangle)$ represents a stimulated one-photon emission (absorption) process. If the coherent evolution starts in $|a\rangle(|c\rangle)$ and ends in $|c\rangle(|a\rangle)$ it represents a two-photon emission (absorption) process.

Therefore, for the *h* and V schemes, the mean change of the probe photon number per period is given by

$$\langle \Delta N_\alpha \rangle^{h,V} = P(a,b)+P(a,c)-P(b,a)-P(c,a), \quad (2)$$

with $P(i,j)$ the probability that a random choice among all coherent evolution periods of the stochastic quantum trajectory gives the period (i,j). For the *p* and Λ schemes, the mean change of the probe photon number per coherent evolution period reads

$$\langle \Delta N_\alpha \rangle^{p,\Lambda} = P(a,b)+P(c,b)-P(b,a)-P(b,c). \quad (3)$$

The physical processes responsible for probe field amplification (absorption) are now one-photon stimulated emission (absorption) and two-photon processes with emission (ab-

sorption) of a probe photon and emission (absorption) for the p scheme and absorption (emission) for the Λ scheme of a drive photon.

Note that the mean change in the probe photon number per unit time relates to the mean change per period as $\langle dN_\alpha/dt\rangle = \langle \Delta N_\alpha\rangle/T$ where T is the average time between two consecutive quantum jumps [see Eqs. (4.11) and (4.16) in Ref. [7]]. In order to evaluate the probability of each one of these coherent evolution periods it is convenient to split the probability $P(i,j)$ into the probability that a coherent evolution period starts in state $|i\rangle$, denoted by $P(i)$, times the conditional probability that a period starting in state $|i\rangle$ ends its coherent evolution in state $|j\rangle$, denoted by $P(j/i)$:

$$P(i,j) = P(i)P(j/i). \tag{4}$$

The probabilities $P(i)$ satisfy the normalization condition $\Sigma_i P(i)=1$. To evaluate these probabilities one needs to make use of the recursive relationship $P(i)=\Sigma_j P(j)Q(i/j)$, where $Q(i/j)$ is the conditional probability of starting a period in state $|i\rangle$ once the previous one started in state $|j\rangle$. These conditional probabilities fulfill the condition $\Sigma_i Q(i/j)=1$ for all j. The explicit values of these conditional probabilities for the four schemes under investigation can be found in Appendix A.

For simplicity, we will restrict ourselves to the case in which there are no dipole dephasing processes, i.e., the so-called radiative limit. In this case $R_{ii}=0$ for all i and atomic dipoles dephase only through the terms R_{ij} (see [16]). Note, however, that the inclusion of R_{ii} in the subsequent results would be straightforward. For the h and V schemes, in the limit $\beta \gg \Sigma_i(R_{bi}+R_{ci}), \Delta_\beta$ and $\alpha \ll \Sigma_i R_{ai}, \beta$, using Eq. (A1) with $R_{ii}=0$ $(i=a,b,c)$, and the former recursive relationship for the probabilities $P(i)$, one obtains

$$P(a)^{h,V} = \frac{(R_{ab}+R_{ac})(R_{ba}+R_{ca})}{D}, \tag{5a}$$

$$P(b)^{h,V} = \frac{R_{ac}R_{cb}+R_{ab}(R_{ba}+R_{ca}+R_{cb})}{D}, \tag{5b}$$

$$P(c)^{h,V} = \frac{R_{ab}R_{bc}+R_{ac}(R_{ba}+R_{ca}+R_{bc})}{D}, \tag{5c}$$

where $D=(R_{ab}+R_{ac})[2(R_{ba}+R_{ca})+R_{bc}+R_{cb}]$. For the p and Λ schemes, in the limit $\beta \gg \Sigma_i(R_{ai}+R_{ci}), \Delta_\beta$ and $\alpha \ll \Sigma_i R_{bi}, \beta$, and using Eq. (A2) with $R_{ii}=0$, one has

$$P(a)^{p,\Lambda} = \frac{R_{ca}(R_{ba}+R_{bc})+R_{ba}(R_{ab}+R_{cb})}{E}, \tag{6a}$$

$$P(b)^{p,\Lambda} = \frac{(R_{ba}+R_{bc})(R_{ab}+R_{cb})}{E}, \tag{6b}$$

$$P(c)^{p,\Lambda} = \frac{R_{ac}(R_{ba}+R_{bc})+R_{bc}(R_{ab}+R_{cb})}{E}, \tag{6c}$$

where $E=(R_{ba}+R_{bc})[2(R_{ab}+R_{cb})+R_{ac}+R_{ca}]$. As stated in Appendix A, the conditional probabilities $Q(i/j)$ and, therefore, the probabilities $P(i)$ given in Eqs. (5) and (6) still remain valid even for a weak driving field provided that (i) R_{bj} for all j or, alternatively, $R_{cj}=0$ for all j (for h and V schemes); or (ii) R_{aj} for all j, or, alternatively, $R_{cj}=0$ for all j (for p and Λ schemes).

On the other hand, the conditional probabilities $P(j/i)$ can be written as [7]

$$P(j/i) = G_j \int_0^\infty |c_{ij}(\tau)|^2 d\tau, \tag{7}$$

where G_j is the departure rate from state $|j\rangle$ of any manifold due to all possible sources of dissipation:

$$G_j = \sum_i R_{ji}, \tag{8}$$

and $c_{ij}(\tau) = \langle j|\exp(-iH_{eff}\tau/\hbar)|i\rangle$ is the probability amplitude to find the system in state $|j\rangle$ at time $t+\tau$ once the coherent evolution period started at time t in state $|i\rangle$ of the same manifold. The effective non-Hermitian Hamiltonian H_{eff} for the four three-level schemes of Fig. 1 can be found in Appendix B. Since $H_{eff}^\dagger = H_{eff}^*$ for all four schemes, the probability amplitudes satisfy the symmetry property

$$c_{ij} = c_{ji}, \tag{9}$$

as shown in Ref. [7].

III. FUNCTIONAL DEFINITION OF THE GENERALIZED EINSTEIN *B* COEFFICIENTS

Once the physical processes responsible for probe amplification or attenuation have been identified and the respective contributions have been calculated, it is straightforward to define in the Einstein spirit four different B coefficients for one- and two-photon gain and loss processes. Thus, for the h and V schemes, a functional definition of these generalized Einstein B coefficients is

$$\left(\frac{d}{dt}n_\alpha\right)^{h,V} = \hbar\omega_\alpha n_\alpha(\rho_{aa}B_{ab}+\rho_{aa}B_{ac}-\rho_{bb}B_{ba}-\rho_{cc}B_{ca}), \tag{10}$$

where n_α is the number of photons per unit volume in the probe mode. $n_\alpha\rho_{aa}B_{ab}$ and $n_\alpha\rho_{bb}B_{ba}$ account for the rates of one-photon gain and loss processes, and $n_\alpha\rho_{aa}B_{ac}$ and $n_\alpha\rho_{cc}B_{ca}$ for two-photon gain and loss processes, respectively. For the p and Λ schemes, this functional definition reads

$$\left(\frac{d}{dt}n_\alpha\right)^{p,\Lambda} = \hbar\omega_\alpha n_\alpha(\rho_{aa}B_{ab}+\rho_{cc}B_{cb}-\rho_{bb}B_{ba}-\rho_{bb}B_{bc}), \tag{11}$$

with $n_\alpha\rho_{aa}B_{ab}$ and $n_\alpha\rho_{bb}B_{ba}$ accounting for the rates of one-photon gain and loss processes, and $n_\alpha\rho_{cc}B_{cb}$ and $n_\alpha\rho_{bb}B_{bc}$ for the rates of two-photon gain and loss processes, respectively.

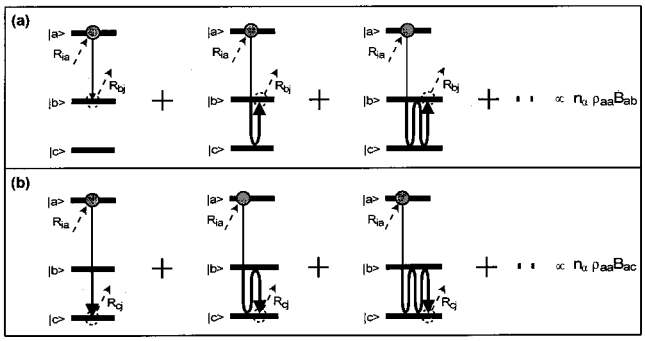

FIG. 3. Schematic respresentation of (a) one-photon gain processes and (b) two-photon gain processes for the *h* scheme of Fig. 1(a). The thin (thick) line represents the interaction with the probe (driving) field. In all three processes shown in (a) the atom undergoes a transition from state $|a\rangle$ to state $|b\rangle$ with an energy exchange between the atom and the fields $\Delta N_\alpha = +1$ and $\Delta N_\alpha = 0$. R_{ia} is a quantum jump that brings the atom to state $|a\rangle$ and R_{bj} a quantum jump that takes the atom out of state $|b\rangle$. (b) The same for two-photon gain processes with R_{cj} a quantum jump that takes the atom out of state $|c\rangle$. $n_\alpha \rho_{aa} B_{ab}$ and $n_\alpha \rho_{aa} B_{ac}$ are the rates of one- and two-photon gain processes, with B_{ab} and B_{ac} the generalized Einstein *B* coefficients for one- and two-photon gain, respectively.

The meaning of these generalized Einstein *B* coefficients can be easily understood with the help of Fig. 3. As shown in Fig. 3(a), the term involving the B_{ab} coefficient accounts for the rate corresponding to the summation of all processes starting in state $|a\rangle$, following a quantum jump given by the incoherent process R_{ia} $(i=a,b,c)$, and ending in state $|b\rangle$ through a quantum jump given by R_{bj} $(j=a,b,c)$. In all these one-photon gain processes the energy exchange between the atom and the two coherent fields satisfies $\Delta N_\alpha = +1$ with $\Delta N_\beta = 0$ irrespective of the explicit number of driving photons involved in the interaction. Figure 3(b) illustrates schematically the meaning of the generalized Einstein B_{ac} coefficient for two-photon gain processes.

In order to motivate interest in these generalized Einstein *B* coefficients, let us consider, for instance, the Λ scheme of Fig. 1(d) for the two following well known cases: (i) $\Delta_\alpha = 0$ with $\Delta_\beta \gg \beta$, and (ii) $\Delta_\alpha = \Delta_\beta \gg \beta$.

In the first case, only one-photon processes take place since two-photon processes are completely detuned from two-photon atomic resonance. The probe attenuation or amplification satisfies

$$\left(\frac{d}{dt} n_\alpha\right)^\Lambda = \hbar \omega_\alpha n_\alpha (\rho_{aa} B_{ab} - \rho_{bb} B_{ba}) = \hbar \omega_\alpha n_\alpha B_{ab} (\rho_{aa} - \rho_{bb}), \tag{12}$$

where we made use of the well known fact that the probabilities for stimulated emission and absorption are equal in this case, i.e., $B_{ab} = B_{ba}$. The former expression simply states that net probe amplification (absorption) occurs for $\rho_{aa} > \rho_{bb}$ $(\rho_{aa} < \rho_{bb})$, and transparency for $\rho_{aa} = \rho_{bb}$. Conventional lasing occurs when the gain associated with the population inversion $(\rho_{aa} - \rho_{bb})$ overcomes cavity losses.

In the second case, only two-photon processes take place in the Λ scheme. The equation that governs probe attenuation or amplification now becomes:

$$\left(\frac{d}{dt} n_\alpha\right)^\Lambda = \hbar \omega_\alpha n_\alpha (\rho_{cc} B_{cb} - \rho_{bb} B_{bc}) = \hbar \omega_\alpha n_\alpha B_{cb} (\rho_{cc} - \rho_{bb}), \tag{13}$$

with $B_{cb} = B_{bc}$ in this case due to the equality between the probabilities for two-photon stimulated emission and absorption. Now, the sign of the two-photon population difference determines the behavior of the medium. For $\rho_{cc} - \rho_{bb} > 0$ (<0) there is net probe amplification (absorption) while probe transparency occurs for $\rho_{cc} = \rho_{bb}$. In fact, the Λ system can operate as a Stokes (or anti-Stokes) Raman laser when a large enough two-photon population inversion occurs.

In these two cases probe amplification or absorption occurs depending on whether there is population inversion or not. Nevertheless, it is well known that three-level systems driven close to resonance, i.e., for $\beta \gg \Delta_\beta$, present unusual features that cannot be explained in terms of population differences alone [17], e.g., coherent population trapping [18], electromagnetically induced transparency [19], amplification or lasing without population inversion [20], and population inversion without amplification or lasing [21]. We are interested here in this laser-matter interaction regime for which both one- and two-photon processes are present at similar rates and where the occurrence of a process or its reverse does not depend only on the population differences between the levels connected. By using the generalized Einstein *B* coefficients defined in Eqs. (10) and (11), we will explicitly demonstrate and quantify a symmetry breaking (i.e., $B_{ij} \neq B_{ji}$) between, on the one hand, one-photon gain and loss processes, and, on the other hand, two-photon gain and loss processes. Simple quantitative expressions for this asymmetry in terms of the incoherent processes present in each particular scheme will be obtained.

IV. RELATIONSHIPS BETWEEN THE GENERALIZED EINSTEIN *B* COEFFICIENTS

Since, on the one hand, expressions (2) and (10) and, on the other hand, expressions (3) and (11), are two different ways of writing the probe attenuation or amplification condition, they must be proportional and, therefore, one has

$$P(i,j) = c \rho_{ii} B_{ij}, \tag{14}$$

with *c* a common constant for all coherent evolution periods of a given quantum trajectory. Substituting Eqs. (4) and (7) in Eq. (14), the generalized Einstein *B* coefficients read

$$B_{ij} = \frac{1}{c} \frac{P(i) G_j}{\rho_{ii}} \int_0^\infty |c_{ij}(\tau)|^2 d\tau. \tag{15}$$

In what follows, and in order to be more specific, we will focus our analysis of these generalized Einstein *B* coeffi-

cients first on the *h* and V schemes and, eventually, we will extend the results to the other two schemes.

A. *h* and V schemes

Using the symmetry property (9), it is straightforward to obtain from Eq. (15) the relationships between the Einstein *B* coefficients for one-photon

$$\frac{B_{ab}}{B_{ba}}=\frac{P(a,b)}{P(b,a)}\frac{\rho_{bb}}{\rho_{aa}}=\frac{P(a)}{P(b)}\frac{G_b}{G_a}\frac{\rho_{bb}}{\rho_{aa}} \tag{16}$$

and two-photon processes

$$\frac{B_{ac}}{B_{ca}}=\frac{P(a,c)}{P(c,a)}\frac{\rho_{cc}}{\rho_{aa}}=\frac{P(a)}{P(c)}\frac{G_c}{G_a}\frac{\rho_{cc}}{\rho_{aa}}. \tag{17}$$

On the other hand, for an intense driving field such that $\beta \gg R_{bc}$, R_{cb}, and Δ_β then transition $|b\rangle$-$|c\rangle$ saturates and, in this case, one has in the steady state

$$\rho_{bb}\simeq\rho_{cc}, \tag{18}$$

while, for a weak probe field, the time evolution of the population of state $|a\rangle$ is governed by

$$\dot{\rho}_{aa}=\sum_{i=b,c}(R_{ia}\rho_{ii}-R_{ai}\rho_{aa}), \tag{19}$$

which, in the steady state and using Eq. (17), gives

$$\rho_{aa}\simeq\frac{R_{ba}+R_{ca}}{R_{ab}+R_{ac}}\rho_{bb.} \tag{20}$$

Let us denote the asymmetry between the Einstein coefficients for, on the one hand, one-photon gain and loss processes, and, on the other hand, two-photon gain and loss processes by $(\Delta B_{1p})^{h,V}$ and $(\Delta B_{2p})^{h,V}$, respectively, in such a way that

$$\frac{B_{ab}}{B_{ba}}=1+(\Delta B_{1p})^{h,V}, \tag{21a}$$

$$\frac{B_{ac}}{B_{ca}}=1+(\Delta B_{2p})^{h,V}. \tag{21b}$$

Using Eqs. (5), (8), and (16)–(21), one obtains

$$(\Delta B_{1p})^{h,V}\simeq\frac{R_{ac}R_{ba}-R_{ab}R_{ca}+(R_{bc}-R_{cb})(R_{ab}+R_{ac})}{R_{cb}(R_{ab}+R_{ac})+R_{ab}(R_{ba}+R_{ca})}, \tag{22a}$$

$$(\Delta B_{2p})^{h,V}\simeq\frac{(R_{cb}-R_{bc})(R_{ab}+R_{ac})-R_{ac}R_{ba}+R_{ab}R_{ca}}{R_{bc}(R_{ab}+R_{ac})+R_{ac}(R_{ba}+R_{ca})}. \tag{22b}$$

Thus, these expressions quantify the asymmetries between the Einstein coefficients for stimulated emission and absorption for one- and two-photon gain and loss processes. Two conclusions come from these two expressions: (i) the particular incoherent processes present in the scheme under consideration and their rate value determine the amount and the sign of these asymmetries for one- and two-photon processes, and (ii) whenever $\Delta B_{1p}>0$ (<0) then $\Delta B_{2p}<0$ (>0) which means that a ''positive'' asymmetry between one-photon gain and loss processes always comes with a ''negative'' asymmetry between two-photon gain and loss processes, and vice versa. Note that, in general, $|(\Delta B_{1p})^{h,V}|\neq|(\Delta B_{2p})^{h,V}|$.

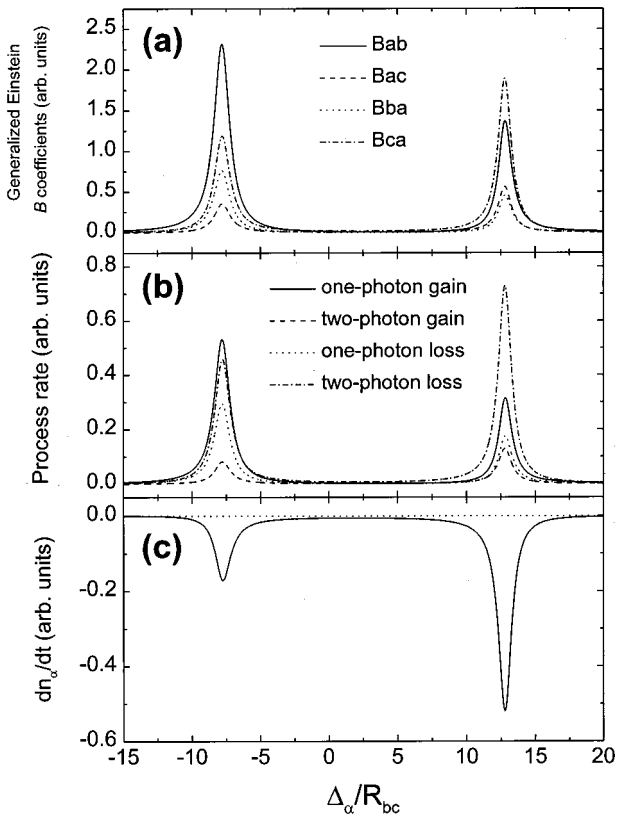

FIG. 4. For the *h* scheme of Fig. 1(a): (a) Relative value of the generalized Einstein *B* coefficients for one-photon gain (B_{ab}), two-photon gain (B_{ac}), one-photon absorption (B_{ba}), and two-photon absorption (B_{ca}); (b) relative value of the rates for one- and two-photon gain and loss processes; and (c) total probe response [see Eq. (15) in the text]. The parameters are $R_{ab}=0.3R_{bc}$, $R_{ba}=0.2R_{bc}$, $R_{ac}=0.2R_{bc}$, $R_{ca}=0.1R_{bc}$, $R_{cb}=0.2R_{bc}$, $R_{aa}=R_{bb}=R_{cc}=0$, $\beta=20R_{bc}$, $\Delta_\beta=-5R_{bc}$, and $\alpha=0.000\,02R_{bc}$.

For the *h* scheme, Fig. 4(a) shows, through a numerical integration of Eq. (15) (see Appendix C), the relative value of the generalized Einstein *B* coefficients as a function of the probe detuning. The parameter setting is $R_{ab}=0.3R_{bc}$, $R_{ba}=0.2R_{bc}$, $R_{ac}=0.2R_{bc}$, $R_{ca}=0.1R_{bc}$, $R_{cb}=0.2R_{bc}$, $\beta=20R_{bc}$, $\Delta_\beta=-5R_{bc}$, and $\alpha=0.000\,02R_{bc}$. For these parameter values the (Δ_α-independent) steady-state populations are $\rho_{aa}\simeq0.23$, $\rho_{bb}\simeq0.36$, and $\rho_{cc}\simeq0.41$. As expected, it is clearly seen in Fig. 4(a) that $\Delta B_{1p}\Delta B_{2p}<0$ and, as predicted by Eqs. (21) and (22), $B_{ab}/B_{ba}\simeq3.2$ and $B_{ac}/B_{ca}\simeq0.27$ for any probe detuning. Figure 4(b) shows the individual contributions of the different physical processes to the probe response (i.e., $\hbar\omega_\alpha n_\alpha\rho_{ii}B_{ij}$, $i\neq j=a,b,c$). The total probe response is plotted in Fig. 4(c) showing the well known Rabi sidebands or Autler-Townes

doublet. Notice that, although there is only absorption in the probe spectrum, for negative detunings the B_{ab} coefficient associated with one-photon gain is the largest. In fact, at the left Rabi sideband, i.e., for $\Delta_\alpha \simeq -7.8R_{bc}$, the main contribution to the right hand side of Eq. (10) is given by one-photon gain processes, while at the right Rabi sideband, i.e., for $\Delta_\alpha \simeq 12.8R_{bc}$, two-photon absorption processes dominate. Finally, we have checked that the probe response shown in Fig. 4(b) completely agrees with a standard density-matrix calculation.

Although we have seen that B_{ab}/B_{ba} and B_{ac}/B_{ca} are fixed by the relaxation rates R_{ij} of the system under consideration, and therefore do not depend on α, Δ_α, β, and Δ_β, the individual Einstein coefficients B_{ij} do indeed depend on these last parameters [as an example of the dependence on Δ_α see Fig. 4(a)]. This dependence can be used to enhance one-photon processes, and simultaneously decrease two-photon processes or vice versa. For instance, in the case of Fig. 4, since $B_{ab} > B_{ba}$ and $B_{ac} < B_{ca}$, to get the maximum probe absorption one must promote two-photon processes at the expense of one-photon processes, and this is achieved by operating near the two-photon resonance condition $\Delta_\alpha \approx -\Delta_\beta$ and far from the one-photon resonance condition $\Delta_\alpha \approx 0$.

In order to further analyze Eqs. (22a) and (22b) let us consider the following simpler cases.

1. Two-photon electric dipole forbidden transition

Let us take transition $|a\rangle$-$|c\rangle$ as an electric dipole forbidden transition such that spontaneous emission from $|a\rangle$ to $|c\rangle$ and incoherent pumping from $|c\rangle$ to $|a\rangle$ can be neglected, i.e., $R_{ac}, R_{ca} \approx 0$. Then, Eqs. (22) read

$$(\Delta B_{1p})^{h,V} \simeq \frac{R_{bc} - R_{cb}}{R_{ba} + R_{cb}}, \tag{23a}$$

$$(\Delta B_{2p})^{h,V} \simeq \frac{R_{cb} - R_{bc}}{R_{bc}}. \tag{23b}$$

Clearly the rate difference $R_{bc} - R_{cb}$ determines the sign of the asymmetry between the generalized Einstein *B* coefficients, and, in particular, for $R_{bc} = R_{cb}$ there is no symmetry breaking. This last case is easily understood by recalling that these rates act on the driven transition and, therefore, determine also if the medium amplifies, absorbs or, for $R_{bc} = R_{cb}$, becomes transparent for the driving field. Thus, for $R_{bc} = R_{cb}$ the driving field does not give rise to any asymmetry in these generalized Einstein *B* coefficients. For $R_{bc} \neq R_{cb}$ the sign of the asymmetries depends on whether the driving field is absorbed or amplified. For the *h* scheme with $R_{bc} > R_{cb}$ ($R_{bc} < R_{cb}$) the driven transition is not inverted (inverted) and then the driving field will be absorbed (amplified). On the contrary, for the V scheme with $R_{bc} > R_{cb}$ ($R_{bc} < R_{cb}$) the driven transition is inverted (not inverted) and, therefore, the driving field will be amplified (absorbed). Thus, what governs the sign of the asymmetry between the Einstein *B* coefficients is the driving field absorption or amplification. Commonly, the driven transition is not inverted and one has then $\Delta B_{1p} > 0$ and $\Delta B_{2p} < 0$ for the *h* scheme and $\Delta B_{1p} < 0$ and $\Delta B_{2p} > 0$ for the V scheme. Note that these last results fully agree with previous discussions in the context of LWI about the origin of inversionless gain and, in particular, about the role played by the incoherent processes coupled to the driven transition [22,10].

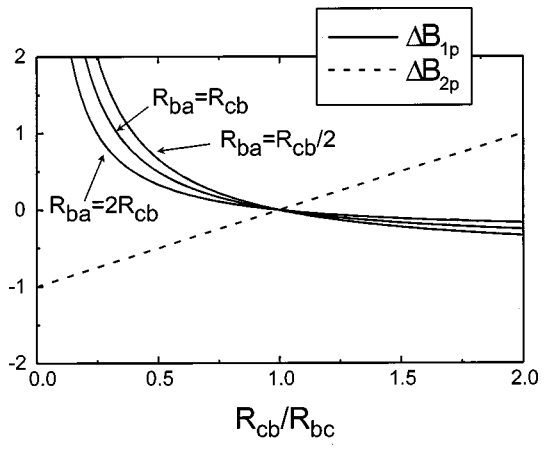

FIG. 5. Asymmetry between the generalized Einstein *B* coefficients for one-photon (ΔB_{1p}) and two-photon processes (ΔB_{2p}) for the *h* scheme with R_{ab}, R_{ba}, R_{ba}, $R_{cb} \neq 0$. The rest of the R_{ij} are taken as identically zero.

As an example, let us consider the *h* scheme with the following incoherent processes: spontaneous emission from $|a\rangle$ to $|b\rangle$ and from $|b\rangle$ to $|c\rangle$, and incoherent pumping from $|b\rangle$ to $|a\rangle$ and from $|c\rangle$ to $|b\rangle$, i.e., R_{ab}, R_{ba}, R_{bc}, $R_{cb} \neq 0$. The rest of the rates R_{ij} are taken identically zero and, therefore, for $R_{ba} > R_{ab}$ ($R_{cb} > R_{bc}$) the probed (driven) transition is inverted. Figure 5 shows the asymmetry between the generalized Einstein *B* coefficients given by Eq. (23). For $R_{cb} = R_{bc}$ there is no symmetry breaking, i.e., $\Delta B_{1p} = \Delta B_{2p} = 0$ since then the medium becomes transparent for the driving field. For $R_{cb} < R_{bc}$ (drive absorption) the generalized Einstein *B* coefficient for one-photon gain overcomes the corresponding one for one-photon loss while for $R_{cb} > R_{bc}$ the generalized *B* coefficient for two-photon gain overcomes that for two-photon loss. Note that these asymmetries do not depend on R_{ab} although the generalized Einstein *B* coefficients and the corresponding rates for one- and two-photon processes depend indeed on R_{ab} through the steady-state populations. For this *h* scheme, Fig. 6(a) shows the relative value of the generalized Einstein *B* coefficients as a function of the probe field detuning for $R_{ab} = 0.1R_{bc}$, $R_{ba} = 0.08R_{bc}$, $\beta = 7R_{bc}$, $\Delta_\beta = 0$, and $\alpha = 0.000\,02R_{bc}$. The rest of the rates are zero. For these parameter settings the steady-state populations are $\rho_{aa} = 0.279$, $\rho_{bb} = 0.349$, and $\rho_{cc} = 0.372$. Equations (21) and (23) now give $B_{ab}/B_{ba} \simeq 13.5$ and $B_{ac}/B_{ca} = 0$ in the whole probe spectrum. In fact, as $R_{cj} = 0$ for all j there are no quantum jumps taking the system out of state $|c\rangle$, which means that there are no two-photon gain processes, i.e., since $G_c = 0$ then $B_{ac} = 0$ [see Eq. (15)]. Figure 6(b) shows the individual contributions of the different physical processes to the probe response. Notice that the main process at and between the Rabi sidebands is two-photon absorption, while at the wings of the Rabi side-

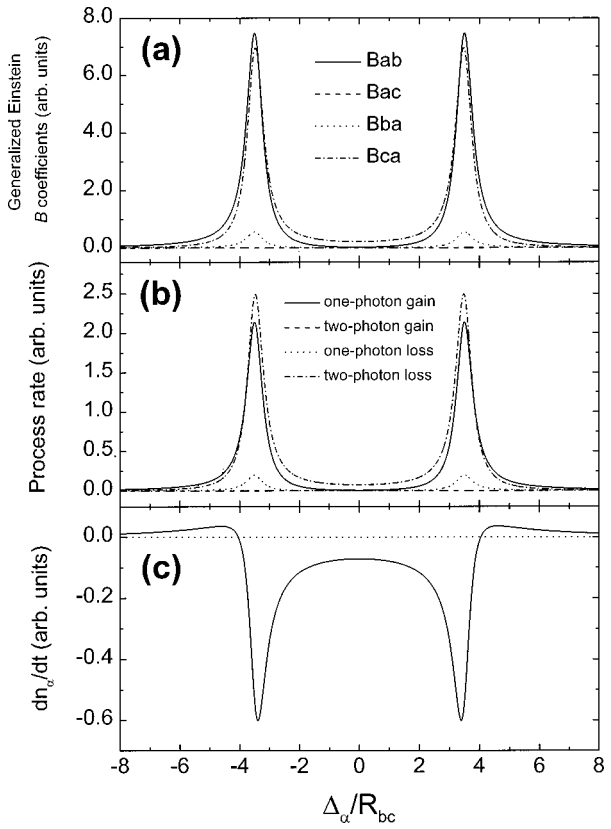

FIG. 6. As in Fig. 4 for the following set of parameters: $R_{ab}=0.1R_{bc}$, $R_{ba}=0.08R_{bc}$, $\beta=7R_{bc}$, $\Delta_\beta=0$, and $\alpha=0.000\,02R_{bc}$. The rest of the R_{ij} are taken as identically zero.

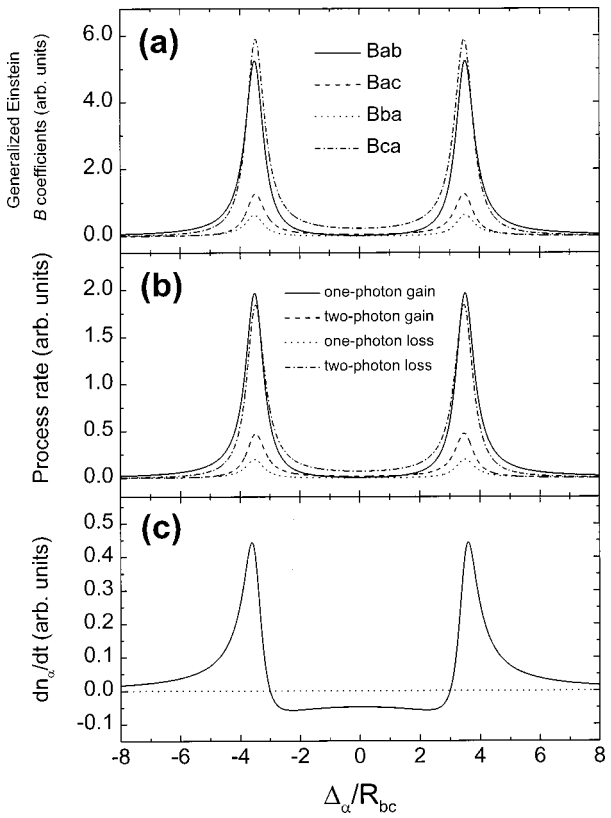

FIG. 7. As in Fig. 4 for the following set of parameters: $R_{ac}=0.1R_{bc}$, $R_{ca}=0.12R_{bc}$, $R_{cb}=0.12R_{bc}$, $\beta=7R_{bc}$, $\Delta_\beta=0$, and $\alpha=0.000\,02R_{bc}$. The rest of the R_{ij} are taken as identically zero.

bands one-photon gain processes predominate even though there is no one-photon inversion. In fact, the total probe response plotted in Fig. 6(c) shows the possibility of inversionless amplification at the wings of the Rabi sidebands. It is worth mentioning that inversionless amplification at these additional sidebands has been previously predicted but still remains to be experimentally observed [10,23].

2. Probing an electric dipole forbidden transition

For a probe field coupling a weak transition, e.g., an electric dipole forbidden transition, we can take $R_{ab},R_{ba}\approx 0$ in Eqs. (22) and then

$$(\Delta B_{1p})^{h,V}\simeq\frac{R_{bc}-R_{cb}}{R_{cb}}, \tag{24a}$$

$$(\Delta B_{2p})^{h,V}\simeq\frac{R_{cb}-R_{bc}}{R_{bc}+R_{ca}}. \tag{24b}$$

As in the previous case, the sign of the asymmetry between one- and two-photon gain and loss processes is governed by the rate difference $R_{bc}-R_{cb}$ that also controls the driving field amplification or absorption.

Again for the *h* scheme, Fig. 7(a) shows the relative value of the generalized Einstein *B* coefficients as a function of the probe detuning for the following parameter values: $R_{ac}=0.1R_{bc}$, $R_{ca}=0.12R_{bc}$, $R_{cb}=0.12R_{bc}$, $\beta=7R_{bc}$, $\Delta_\beta=0$, and $\alpha=0.000\,02R_{bc}$. The steady-state populations read now $\rho_{aa}\simeq 0.378$, $\rho_{bb}\simeq 0.308$, and $\rho_{cc}\simeq 0.315$, i.e., since $R_{ca}>R_{ac}$ there is one-photon ($\rho_{aa}>\rho_{bb}$) and two-photon ($\rho_{aa}>\rho_{cc}$) population inversion. The ratio between the Einstein *B* coefficients reads $B_{ab}/B_{ba}=8.3$ and $B_{ac}/B_{ca}=0.21$. Notice in Fig. 7(b) that two-photon absorption is the main process between the Rabi sidebands in spite of the fact that there is two-photon population inversion. In fact, the total probe response plotted in Fig. 7(c) shows absorption between the Rabi sidebands. It is worth mentioning that this so-called population inversion without amplification or lasing based on two-photon absorption was proposed very recently as an alternative method to *Q* switching in order to generate giant pulses of laser light [24]. In fact, we see in Fig. 7(c) that there is probe absorption at $|\Delta_\alpha|\lesssim 3R_{bc}$ in the presence of population inversion at the $|a\rangle\rightarrow|b\rangle$ transition. It is possible to extract the energy from this inverted transition in the form of a laser pulse by switching off the drive field in the other transition [24].

3. Driving an electric dipole forbidden transition

Let us consider now a drive field acting on a dipole forbidden transition. In this case, we can take $R_{bc},R_{cb}\approx 0$ in Eqs. (22) and therefore

$$(\Delta B_{1p})^{h,V}\simeq\frac{R_{ac}R_{ba}-R_{ab}R_{ca}}{R_{ab}(R_{ba}+R_{ca})}, \tag{25a}$$

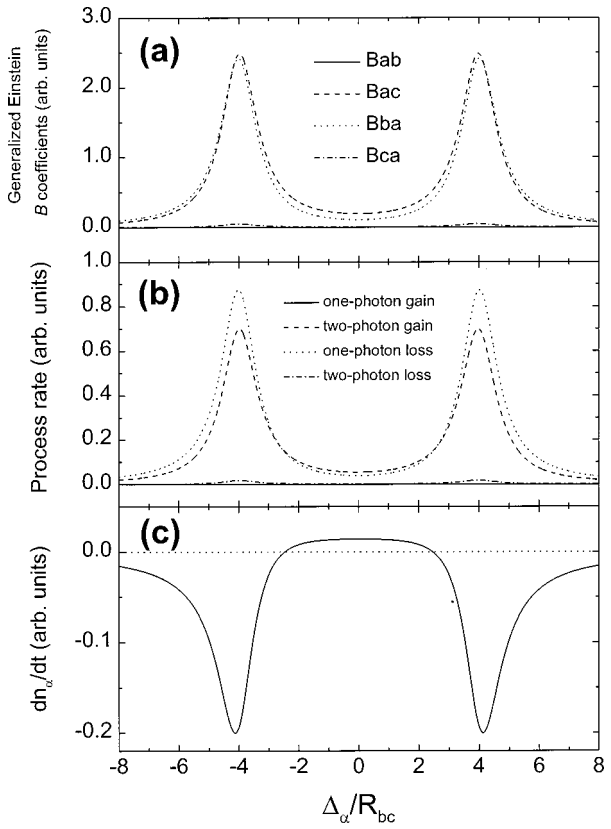

FIG. 8. As in Fig. 4 for the following set of parameters: $R_{ac}=0.02R_{ab}$, $R_{ca}=0.8R_{ab}$, $\beta=8R_{ab}$, $\Delta_\beta=0$, and $\alpha=0.000\,02R_{ab}$. The rest of the R_{ij} are taken as identically zero.

$$(\Delta B_{2p})^{h,V}\simeq\frac{R_{ab}R_{ca}-R_{ac}R_{ba}}{R_{ac}(R_{ba}+R_{ca})}. \tag{25b}$$

The rate difference $R_{ac}R_{ba}-R_{ab}R_{ca}$ now determines the sign of the symmetry breakings. Moreover, one can increase one-photon gain asymmetry $(\Delta B_{1p})^{h,V}$ by taking, for instance, $R_{ab}\to 0$, or, alternatively, two-photon gain asymmetry $(\Delta B_{2p})^{h,V}$, for $R_{ac}\to 0$. Note, however, that these rates control also whether there is inversion or not in the probed transition. In particular, from Eq. (20) for $R_{ab}+R_{ac}<R_{ba}+R_{ca}$ the probed transition is inverted.

For the *h* scheme, Fig. 8 shows the relative value of the *B* coefficients for the following parameter settings: $R_{ac}=0.02R_{ab}$, $R_{ca}=0.8R_{ab}$, $\beta=8R_{ab}$, $\Delta_\beta=0$, and $\alpha=0.000\,02R_{ab}$. For these values the steady-state populations read $\rho_{aa}\simeq 0.281$, $\rho_{bb}\simeq 0.361$, and $\rho_{cc}\simeq 0.358$. Therefore, there is neither one-photon nor two-photon population inversion. The ratio between the Einstein *B* coefficients reads now $B_{ab}/B_{ba}=0$ and $B_{ac}/B_{ca}=51$. One has $B_{ab}=0$ because there are no dissipative processes taking the system out of state $|b\rangle$. Notice in Fig. 8(b) that two-photon gain is the main process between the Rabi sidebands even though there is no two-photon population inversion. In fact, the total probe response plotted in Fig. 8(c) shows amplification without population inversion between the Rabi sidebands. Note that this inversionless gain between the Rabi resonances due to two-photon gain has been observed experimentally very recently in a V type system in laser cooled Rb atoms [25].

B. *p* and Λ schemes

From Eqs. (14) and (15), and using (9), the ratio between the generalized Einstein *B* coefficients for one-photon processes reads now

$$\frac{B_{ab}}{B_{ba}}=\frac{P(a,b)}{P(b,a)}\frac{\rho_{bb}}{\rho_{aa}}=\frac{P(a)}{P(b)}\frac{G_b}{G_a}\frac{\rho_{bb}}{\rho_{aa}}, \tag{26}$$

and for two-photon processes

$$\frac{B_{cb}}{B_{bc}}=\frac{P(c,b)}{P(b,c)}\frac{\rho_{bb}}{\rho_{cc}}=\frac{P(c)}{P(b)}\frac{G_b}{G_c}\frac{\rho_{bb}}{\rho_{cc}}. \tag{27}$$

On the other hand, the steady-state populations read for these schemes

$$\rho_{cc}\simeq\rho_{aa}, \tag{28a}$$

$$\rho_{bb}\simeq\frac{R_{ab}+R_{ab}}{R_{ba}+R_{bc}}\rho_{aa}, \tag{28b}$$

which gives

$$(\Delta B_{1p})^{p,\Lambda}\simeq\frac{R_{ba}R_{cb}-R_{ab}R_{bc}+(R_{ca}-R_{ac})(R_{ba}+R_{bc})}{(R_{ab}+R_{ac})(R_{ba}+R_{bc})}, \tag{29a}$$

$$(\Delta B_{2p})^{p,\Lambda}\simeq\frac{R_{ab}R_{bc}-R_{ba}R_{cb}+(R_{ac}-R_{ca})(R_{ba}+R_{bc})}{(R_{ca}+R_{cb})(R_{ba}+R_{bc})}. \tag{29b}$$

Again, the generalized Einstein *B* coefficients satisfy $\Delta B_{1p}\Delta B_{2p}\leqslant 0$ with, in general, $|\Delta B_{1p}|\neq|\Delta B_{2p}|$. As was done previously, we will analyze these expressions for the following three simpler cases.

1. Two-photon electric dipole forbidden transition

In this case we take $R_{bc},R_{cb}\approx 0$ and thus

$$(\Delta B_{1p})^{p,\Lambda}\simeq\frac{R_{ca}-R_{ac}}{R_{ab}+R_{ac}}, \tag{30a}$$

$$(\Delta B_{2p})^{p,\Lambda}\simeq\frac{R_{ac}-R_{ca}}{R_{ca}}. \tag{30b}$$

Again, the incoherent processes present in the driven transition determine the sign of the one-photon and two-photon asymmetries.

2. Probing an electric dipole forbidden transition

Taking $R_{ab},R_{ba}\approx 0$ Eqs. (29) become

$$(\Delta B_{1p})^{p,\Lambda}\simeq\frac{R_{ca}-R_{ac}}{R_{ac}}, \tag{31a}$$

$$(\Delta B_{2p})^{p,\Lambda} \simeq \frac{R_{ac}-R_{ca}}{R_{ca}+R_{cb}}. \tag{31b}$$

As in the previous case, the rate difference $R_{ca}-R_{ac}$ determines the sign of the asymmetries.

3. Driving an electric dipole forbidden transition

Finally, in this case one has $R_{ac}, R_{ca} \approx 0$ and thus

$$(\Delta B_{1p})^{p,\Lambda} \simeq \frac{R_{ba}R_{cb}-R_{ab}R_{bc}}{R_{ab}(R_{ba}+R_{bc})}, \tag{32a}$$

$$(\Delta B_{2p})^{p,\Lambda} \simeq \frac{R_{ab}R_{bc}-R_{ba}R_{cb}}{R_{cb}(R_{ba}+R_{bc})}. \tag{32b}$$

Now, the rate difference $R_{ba}R_{cb}-R_{ab}R_{bc}$ determines the sign of the one-photon and two-photon asymmetries. It is possible to enhance one-photon gain asymmetry by taking $R_{ab} \to 0$ or, alternatively, two-photon gain asymmetry by taking $R_{cb} \to 0$.

V. CONCLUSIONS

We have analyzed closed three-level schemes driven near resonance on one transition by an intense TW laser field while probed at an adjacent transition by a weak TW laser field. We have made use of the quantum-jump formalism to identify and quantify the different physical processes responsible for probe amplification or absorption. By using this technique, we have defined generalized Einstein *B* coefficients for one- and two-photon gain and loss processes showing that, in general, these generalized *B* coefficients are different for stimulated emission and absorption both for one-photon processes and for two-photon processes. We have obtained simple analytical expressions for these asymmetries between generalized Einstein coefficients for one- and two-photon processes in terms of the rates of the particular incoherent processes present in each scheme. Some general properties of these generalized Einstein *B* coefficients have been found, e.g., a ''positive'' asymmetry between the coefficients for one-photon processes always comes together with a ''negative'' asymmetry between the coefficients for two-photon processes, and vice versa. All these analytical results have been tested by a numerical calculation of the relative value of these generalized Einstein *B* coefficients. In addition, it has also been verified that the probe response given by these *B* coefficients completely agrees with that obtained from a standard density-matrix analysis. Finally, some very well known phenomena occurring in coherently driven three-level systems, such as amplification without inversion or inversion without amplification, have been discussed in terms of the asymmetries between these generalized Einstein *B* coefficients.

An extension of the analysis presented in this paper to open or multilevel systems is straightforward provided that the required conditions mentioned in the Introduction for the applicability of the quantum-jump technique are satisfied. However, it seems more difficult to obtain analytical expressions for the relative value of these generalized Einstein *B* coefficients in the presence of a standing wave drive configuration. In this case, it is well known that the number of system states belonging to a given manifold is infinite [26] which avoids the possibility of using the analytical tools reviewed in Sec. II. Instead, it is possible to compute the relative value of these *B* coefficients by performing a numerical analysis of the corresponding quantum-trajectory realizations or Monte Carlo simulations.

ACKNOWLEDGMENTS

Support by the DGICYT (Spanish Government), under Contract No. PB95-0778-C02-02 and PB98-0935-C03-03, and by the DGR (Catalan Government), under Contract No. 1999SGR00096, is acknowledged.

APPENDIX A

In the limit $\beta \gg \Sigma_i(R_{bi}+R_{ci}), \Delta_\beta$ and $\alpha \ll \Sigma_i R_{ai}, \beta$, the conditional probabilities $Q(j/i)$ to start a coherent evolution period in state $|j\rangle$ once the previous one started in $|i\rangle$ can be easily obtained by a simple examination of Fig. 2 for the *h* scheme and of the corresponding figures for other three-level systems. For the *h* scheme (and also for the V scheme) and due to the fact that $\alpha \ll \Sigma_i R_{ai}$ whenever the system starts its coherent evolution in state $|a\rangle$ there will almost always be a quantum jump from this state $|a\rangle$ to other states before the amplitude probability to be in state $|b\rangle$ or $|c\rangle$ becomes significant. Then,

$$Q(a/a)^{h,V} = R_{aa}/(R_{aa}+R_{ab}+R_{ac}), \tag{A1a}$$

$$Q(b/a)^{h,V} = R_{ab}/(R_{aa}+R_{ab}+R_{ac}), \tag{A1b}$$

$$Q(c/a)^{h,V} = R_{ac}/(R_{aa}+R_{ab}+R_{ac}). \tag{A1c}$$

On the other hand, since $\beta \gg \Sigma_i(R_{bi}+R_{ci}), \Delta_\beta$, then whenever the system starts its coherent evolution in state $|b\rangle$ it will evolve in a Rabi oscillatory fashion between $|b\rangle$ and $|c\rangle$ with, on average, half of the time in state $|b\rangle$ and half of the time in state $|c\rangle$, before a quantum jump takes place. Therefore,

$$Q(a/b)^{h,V} = \frac{R_{ba}+R_{ca}}{R_{ba}+R_{ca}+R_{bb}+R_{cb}+R_{bc}+R_{cc}}, \tag{A1d}$$

$$Q(b/b)^{h,V} = \frac{R_{bb}+R_{cb}}{R_{ba}+R_{ca}+R_{bb}+R_{cb}+R_{bc}+R_{cc}}, \tag{A1e}$$

$$Q(c/b)^{h,V} = \frac{R_{bc}+R_{cc}}{R_{ba}+R_{ca}+R_{bb}+R_{cb}+R_{bc}+R_{cc}}, \tag{A1f}$$

and exactly the same if the system starts its coherent evolution in $|c\rangle$:

$$Q(a/c)^{h,V} = \frac{R_{ba}+R_{ca}}{R_{ba}+R_{ca}+R_{bb}+R_{cb}+R_{bc}+R_{cc}}, \tag{A1g}$$

$$Q(b/c)^{h,V}=\frac{R_{bb}+R_{cb}}{R_{ba}+R_{ca}+R_{bb}+R_{cb}+R_{bc}+R_{cc}}, \tag{A1h}$$

$$Q(c/c)^{h,V}=\frac{R_{bc}+R_{cc}}{R_{ba}+R_{ca}+R_{bb}+R_{cb}+R_{bc}+R_{cc}}. \tag{A1i}$$

Notice that Eqs. (A1d)–(A1i) remain valid even for a weak driving field provided that $R_{bj}=0$ for all j (or, alternatively, $R_{cj}=0$ for all j), since then the system cannot leave any multiplicity ξ from state $|b\rangle$ (or, alternatively, from state $|c\rangle$).

For the p and Λ schemes in the limit $\beta \gg \Sigma_i(R_{ai}+R_{ci}), \Delta_\beta$ and $\alpha \ll \Sigma_i R_{bi}, \beta$, these conditional probabilities read

$$Q(a/b)^{p,\Lambda}=R_{ba}/(R_{ba}+R_{bb}+R_{bc}), \tag{A2a}$$

$$Q(b/b)^{p,\Lambda}=R_{bb}/(R_{ba}+R_{bb}+R_{bc}), \tag{A2b}$$

$$Q(c/b)^{p,\Lambda}=R_{bc}/(R_{ba}+R_{bb}+R_{bc}), \tag{A2c}$$

$$Q(a/a)^{p,\Lambda}=Q(a/c)^{p,\Lambda}=\frac{R_{aa}+R_{ca}}{R_{aa}+R_{ca}+R_{ab}+R_{cb}+R_{ac}+R_{cc}}, \tag{A2d}$$

$$Q(b/a)^{p,\Lambda}=Q(b/c)^{p,\Lambda}=\frac{R_{ab}+R_{cb}}{R_{aa}+R_{ca}+R_{ab}+R_{cb}+R_{ac}+R_{cc}}, \tag{A2e}$$

$$Q(c/a)^{p,\Lambda}=Q(c/c)^{p,\Lambda}=\frac{R_{ac}+R_{cc}}{R_{aa}+R_{ca}+R_{ab}+R_{cb}+R_{ac}+R_{cc}}. \tag{A2f}$$

In this case, Eqs. (A2d)–(A2f) are still valid for a weak driving field provided that $R_{aj}=0$ for all j or, alternatively, $R_{cj}=0$ for all j.

Finally, note that the conditional probabilities given in Eqs. (A1) and (A2) do not depend on the laser parameters β, Δ_β, α, and Δ_α, and, consequently, neither will the probabilities $P(i)$ obtained from the recursive relationship $P(i)=\Sigma_j P(j)Q(i/j)$ depend on these parameters.

APPENDIX B

The effective non-Hermitian Hamiltonians for the four three-level schemes under investigation are [7]

$$H_{eff}^{h}=\hbar\begin{pmatrix} -(\Delta_\alpha+\Delta_\beta)-i\frac{G_a}{2} & \alpha/2 & 0 \\ \alpha/2 & -\Delta_\beta-i\frac{G_b}{2} & \beta/2 \\ 0 & \beta/2 & -i\frac{G_c}{2} \end{pmatrix}, \tag{B1a}$$

$$H_{eff}^{V}=\hbar\begin{pmatrix} -\Delta_\alpha-i\frac{G_a}{2} & \alpha/2 & 0 \\ \alpha/2 & -i\frac{G_b}{2} & \beta/2 \\ 0 & \beta/2 & -\Delta_\beta-i\frac{G_c}{2} \end{pmatrix}, \tag{B1b}$$

$$H_{eff}^{p}=\hbar\begin{pmatrix} -\Delta_\alpha-i\frac{G_a}{2} & \alpha/2 & \beta/2 \\ \alpha/2 & -i\frac{G_b}{2} & 0 \\ \beta/2 & 0 & -(\Delta_\alpha+\Delta_\beta)-i\frac{G_c}{2} \end{pmatrix}, \tag{B1c}$$

and

$$H_{eff}^{\Lambda}=\hbar\begin{pmatrix} -\Delta_\beta-i\frac{G_a}{2} & \alpha/2 & \beta/2 \\ \alpha/2 & (\Delta_\alpha-\Delta_\beta)-i\frac{G_b}{2} & 0 \\ \beta/2 & 0 & -i\frac{G_c}{2} \end{pmatrix}. \tag{B1d}$$

APPENDIX C

For the *h* scheme, the time evolution of the complex amplitude probabilities $c_{ij}(\tau)=x_{ij}(\tau)+iy_{ij}(\tau)$ is determined by the Hamiltonian given in Eq. (B1a) and reads

$$\dot{x}_{aa}=-\frac{G_a}{2}x_{aa}-(\Delta_\alpha+\Delta_\beta)y_{aa}+\frac{\alpha}{2}y_{ab}, \tag{C1a}$$

$$\dot{y}_{aa}=-\frac{G_a}{2}y_{aa}+(\Delta_\alpha+\Delta_\beta)x_{aa}-\frac{\alpha}{2}x_{ab}, \tag{C1b}$$

$$\dot{x}_{bb}=-\frac{G_b}{2}x_{bb}-\Delta_\beta y_{bb}+\frac{\alpha}{2}y_{ab}+\frac{\beta}{2}y_{bc}, \tag{C1c}$$

$$\dot{y}_{bb}=-\frac{G_b}{2}y_{bb}+\Delta_\beta x_{bb}-\frac{\alpha}{2}x_{ab}-\frac{\beta}{2}x_{bc}, \tag{C1d}$$

$$\dot{x}_{cc}=-\frac{G_c}{2}x_{cc}+\frac{\beta}{2}y_{bc}, \tag{C1e}$$

$$\dot{y}_{cc}=-\frac{G_c}{2}y_{cc}-\frac{\beta}{2}x_{bc}, \tag{C1f}$$

$$\dot{x}_{ab}=-\frac{G_b}{2}x_{ab}-\Delta_\beta y_{ab}+\frac{\alpha}{2}y_{aa}+\frac{\beta}{2}y_{ac}, \tag{C1g}$$

$$\dot{y}_{ab} = -\frac{G_b}{2} y_{ab} + \Delta_\beta x_{ab} - \frac{\alpha}{2} x_{aa} - \frac{\beta}{2} x_{ac}, \tag{C1h}$$

$$\dot{x}_{ac} = -\frac{G_c}{2} x_{ac} + \frac{\beta}{2} y_{ab}, \tag{C1i}$$

$$\dot{y}_{ac} = -\frac{G_c}{2} y_{ac} - \frac{\beta}{2} x_{ab}, \tag{C1j}$$

$$\dot{x}_{bc} = -\frac{G_c}{2} x_{bc} + \frac{\beta}{2} y_{bb}, \tag{C1k}$$

$$\dot{y}_{bc} = -\frac{G_c}{2} y_{bc} - \frac{\beta}{2} x_{bb}, \tag{C1l}$$

where we have made use of Eq. (9) and $G_a = R_{aa} + R_{ab} + R_{ac}$, $G_b = R_{ba} + R_{bb} + R_{bc}$, and $G_c = R_{ca} + R_{cb} + R_{cc}$. In order to calculate the B_{ij} coefficients given in Eq. (15) we have integrated Eqs. (C1a)–(C1l) by using a Runge-Kutta-Fehlberg routine of orders seventh to eighth and then divided the result by the corresponding atomic population. Note that, due to the presence of dissipation, $x_{ij}(\tau), y_{ij}(\tau) \to 0$ in an exponential way which, in fact, guarantees the convergence of $\int_0^\infty |c_{ij}(\tau)|^2 d\tau$.

[1] A. Einstein, Verh. Dtsch. Phys. Ges. **18**, 318 (1916); Phys. Z. **18**, 121 (1917).
[2] H. J. Carmichael (unpublished).
[3] J. Dalibard, Y. Castin, and K. Mølmer, Phys. Rev. Lett. **68**, 580 (1992).
[4] R. Dum, P. Zoller, and H. Ritsch, Phys. Rev. A **45**, 4879 (1992).
[5] K. Mølmer, Y. Castin, and J. Dalibard, J. Opt. Soc. Am. B **10**, 524 (1993).
[6] A. Imamoglu and L. You, Phys. Rev. A **50**, 2642 (1994); Y. Castin, K. Berg-Sorensen, J. Dalibard, and K. Mølmer, *ibid.* **50**, 5092 (1994); Y. Castin and K. Mølmer, Phys. Rev. Lett. **74**, 3772 (1995); T. Hiroshima and Y. Yamamoto, Phys. Rev. A **56**, 3077 (1997); T. B. L. Kist, A. Z. Khoury, and Davidovich , *ibid.* **54**, 2510 (1996); A. Z. Khoury and T. B. L. Kist, *ibid.* **55**, 2304 (1996); S. Bay, P. Lambropoulos, and K. Molmer, Phys. Rev. Lett. **79**, 2654 (1997).
[7] C. Cohen-Tannoudji, B. Zambon, and E. Arimondo, J. Opt. Soc. Am. B **10**, 2107 (1993).
[8] C. Cohen-Tannoudji and J. Dalibard, Europhys. Lett. **1**, 441 (1986).
[9] E. Arimondo, Proc. SPIE **1726**, 484 (1992).
[10] J. Mompart and R. Corbalán, Opt. Commun. **156**, 133 (1998).
[11] J. Mompart, V. Ahufinger, F. Silva, R. Corbalán, and R. Vilaseca, Laser Phys. **9**, 858 (1999).
[12] These results hold for the usual case in which the driven transition is not inverted (see [10]).
[13] H. J. Carmichael, Phys. Rev. A **56**, 5065 (1997).
[14] A. S. Zibrov, M. D. Lukin, D. E. Nikonov, L. Hollberg, M. O. Scully, V. L. Velichansky, and H. G. Robinson, Phys. Rev. Lett. **75**, 1499 (1995).
[15] F. B. de Jong, R. J. C. Spreeuw, and H. B. van Linden van den Heuvell, Phys. Rev. A **55**, 3918 (1997).
[16] J. Mompart and R. Corbalán, Eur. Phys. J. D **5**, 351 (1999).
[17] A. Javan, Phys. Rev. **107**, 1579 (1957).
[18] E. Arimondo, *Coherent Population Trapping in Laser Spectroscopy*, Vol. 15 in *Progress in Optics*, edited by E. Wolf (Elsevier Science, Amsterdam, 1996).
[19] S. E. Harris, Phys. Today **50** (7), 36 (1997).
[20] O. Kocharovskaya, Phys. Rep. **219**, 175 (1992); M. O. Scully, *ibid.* **219**, 191 (1992); P. Mandel, Contemp. Phys. **34**, 235 (1993); J. Mompart and R. Corbalán, J. Opt. B: Quantum Semiclassical Opt. **2**, R7 (2000).
[21] C. Peters and W. Lange, Appl. Phys. B: Lasers Opt. **62**, 221 (1996); J. Mompart, R. Corbalán, and R. Vilaseca, Phys. Rev. A **59**, 3038 (1998).
[22] P. Mandel and O. Kocharovskaya, Phys. Rev. A **46**, 2700 (1992).
[23] J. Mompart, C. Peters, and R. Corbalán, Phys. Rev. A **57**, 2163 (1998).
[24] J. Mompart, R. Corbalán, and R. Vilaseca, Phys. Rev. A **59**, 3038 (1999).
[25] J. Kitching and L. Hollberg, Phys. Rev. A **59**, 4685 (1999).
[26] L. Roso, R. Corbalán, G. Orriols, R. Vilaseca, and E. Arimondo, Appl. Phys. B: Photophys. Laser Chem. **31**, 115 (1983).